



Overexpression of miR-328-5p influences cell growth and migration to promote NSCLC progression by targeting LOXL4

Yanzhao Ji^{1,2#}, Yanting You^{1#}, Yifen Wu^{3#}, Min Wang⁴, Qiuxing He¹, Xinghong Zhou¹, Liqian Chen¹, Xiaomin Sun¹, Yanyan Liu¹, Xiuqiong Fu⁵, Hiu Yee Kwan⁵, Qiang Zuo⁶, Ren Luo¹, Xiaoshan Zhao¹

¹Syndrome Laboratory of Integrated of Chinese and Western Medicine, School of Chinese Medicine, Southern Medical University, Guangzhou, China; ²Department of Nephrology, Shanxi Bethune Hospital, Shanxi Academy of Medical Science, Taiyuan, China; ³Department of Oncology, Affiliated Dongguan People's Hospital, Southern Medical University, Dongguan, China; ⁴Department of Traditional Chinese Medicine, Zhujiang Hospital of Southern Medical University, Guangzhou, China; ⁵School of Chinese Medicine, Hong Kong Baptist University, Hong Kong, China; ⁶Department of Oncology, Nanfang Hospital, Southern Medical University, Guangzhou, China

Contributions: (I) Conception and design: X Zhao, R Luo; (II) Administrative support: X Zhao, R Luo; (III) Provision of study materials or patients: X Zhao, R Luo; (IV) Collection and assembly of data: Y You, Y Wu, L Chen, Q Zuo; (V) Data analysis and interpretation: Y Ji, M Wang; (VI) Manuscript writing: All authors; (VII) Final approval of manuscript: All authors.

[#]These authors contributed equally to this work.

Correspondence to: Xiaoshan Zhao. Syndrome Laboratory of Integrated of Chinese and Western Medicine, School of Chinese Medicine, Southern Medical University, Guangzhou 510515, China. Email: zhaosx0609@163.com; Ren Luo. Syndrome Laboratory of Integrated of Chinese and Western Medicine, School of Chinese Medicine, Southern Medical University, Guangzhou 510515, China. Email: luoren_2014@outlook.com.

Background: Lung cancer is the leading cause of cancer-associated mortality worldwide, and most lung cancers are classified as non-small cell lung cancer (NSCLC). MiR-328 influence the progression of multiple tumors, but the role of miR-328-5p in NSCLC has not been elucidated. The aim of this study was to illuminate the oncogenic role and potential molecular mechanisms of the miR-328-5p and lysyl oxidase like 4 (LOXL4) in NSCLC.

Methods: Expression of miR-328-5p was detected by real-time quantitative polymerase chain reaction (qRT-PCR) in tumor and non-tumor adjacent tissues. After Lentivirus-miR-328-5p was employed to intervene this miRNA in NSCLC cell lines, RT-qPCR was used to detect the expression levels of miR-328-5p. Cell Counting Kit-8 (CCK-8), cell colony formation, flow cytometry, wound healing, Transwell assays were used to determine the malignant phenotypes of NSCLC cells. Nude mice models of subcutaneous tumors were established to observe the effect of miR-328-5p on tumorigenesis. Targeting the 3'UTR of LOXL4 by miR-328-5p was verified by integrated analysis including transcriptome sequencing, dual-luciferase and western-blot assays.

Results: High miR-328-5p level was observed in NSCLC cells from The Cancer Genome Atlas (TCGA) database and tumor tissues collected from NSCLC patients. Overexpressed miR-328-5p promoted NSCLC cell proliferation, survival, and migration, and promoted tumor growth *in vivo*. Knockdown of miR-328-5p suppressed tumorigenic activities. Transcriptome sequencing analysis revealed that LOXL4 was downregulated by miR-328-5p, which was confirmed by dual-luciferase reporter and western-blot assays.

Conclusions: miR-328-5p showed targeted regulation of LOXL4 to promote cell proliferation and migration in NSCLC.

Keywords: Non-small cell lung cancer (NSCLC); miR-328-5p; lysyl oxidase like 4 (LOXL4)

Submitted Jan 07, 2022. Accepted for publication Feb 21, 2022.

doi: 10.21037/atm-22-345

View this article at: <https://dx.doi.org/10.21037/atm-22-345>

Introduction

With a high incidence and poor survival rates, lung cancer has been the leading cause of cancer-associated mortality worldwide. More than 80% of lung cancers are classified as non-small cell lung cancer (NSCLC). NSCLC can be divided into 2 major categories, namely squamous cell carcinoma and adenocarcinoma (1,2). Although chemotherapy, molecular targeted therapy, and immunotherapy have made promising advances in NSCLC treatment, the overall clinical outcomes are poor, with unfavorable prognosis and increased risk of treatment-related complications (3,4). In China, compared to most countries, the incidence and mortality of NSCLC are relatively high, causing enormous harm to human health (2,5), and poor areas still account for the dominant proportion of NSCLC cases in China (6). It is projected that the rate of NSCLC deaths in China may increase to approximately 40% in 2030 (7). Thus, there is an urgent need to find novel diagnostic and prognostic biomarkers for NSCLC.

MicroRNAs (miRNAs) are endogenous, highly conserved, single-stranded, non-coding small RNAs 18–23 nucleotides in length (8). They can lead to various diseases by binding specifically to the 3'-non-coding region of the antisense strand of the target gene (9). Increasing evidence has shown that miRNAs play an important role in regulating the progression of NSCLC (10–12). MiR-328 has been reported to function as a cancer-related miRNA. MiR-328 could increase reactive oxygen species (ROS) production and promote the adhesion and migration ability of monocytes during monocyte maturation (13). In lung cancer, miR-328 expression was significantly elevated and could promote cell migration (14–16).

In the present study, we found that the expression of miR-328-5p was upregulated in primary tumor tissues from NSCLC patients compared with adjacent tissues, and overexpression of miR-328-5p promoted NSCLC cell proliferation and migration. These results suggested that miR-328-5p may be a tumor promoter in NSCLC. We also demonstrated that miR-328-5p could directly bind to lysyl oxidase like 4 (LOXL4). This suggests that miR-328-5p may promote NSCLC cell proliferation and migration through targeted inhibition of LOXL4 expression. Taken together, these findings revealed that miR-328-5p/LOXL4 play a crucial role in NSCLC progression and highlight that miR-328-5p could be a potential biomarker for the diagnosis of NSCLC. We present the following article in

accordance with the ARRIVE reporting checklist (available at <https://atm.amegroups.com/article/view/10.21037/atm-22-345/rc>).

Methods

Patients and tissue collection

Thirty paraffin-embedded lung cancer tissues and 30 pair-matched adjacent normal tissues were collected, along with the clinical data of the patients. The study was conducted in accordance with the Declaration of Helsinki (as revised in 2013). The study was approved by the Ethics Committee of Nanfang Hospital and informed consent was taken from all the patients.

Total RNA isolation, miRNA isolation, and qRT-PCR

MiRNA was extracted from paraffin-embedded tissues using a Rapid microRNA Extraction Kit (centrifugal column type) (Beijing Baitaike Biotechnology Co., Ltd., China), and total RNA containing miRNA was extracted from cell lines using RNAiso Plus reagent (TaKaRa, Japan). The reverse transcription reaction was performed using the All-in-One™ First-Strand cDNA Synthesis Kit (GeneCopoeia™, Guangzhou, China). We performed real-time quantitative polymerase chain reaction (qRT-PCR) on a 7500 Real-time PCR System (Applied Biosystems, Foster City, CA, USA) using the All-in-One™ miRNA qRT-PCR Detection Kit (GeneCopoeia™) following the manufacturer's protocol. The primers for *miR-328-5p* were designed by GeneCopoeia™. MiRNA expression was normalized to *U6*. Each sample was tested in triplicate.

Culture of lung cancer cells

Human A549 and SPC-A1 cells were maintained in Dulbecco's modified Eagle's medium (Gibco) supplemented with 10% fetal bovine serum (FBS; Gibco), 100 U/mL penicillin, and 100 mg/mL streptomycin at 37 °C with 5% CO₂.

MiR-328-5p modification in lung cancer cells

Lentiviral vectors were used to establish stable overexpression (LV-328-5p-m), inhibition (LV-328-5p-i), and negative control (LV-NC) NSCLC cells (obtained from GenePharma, Shanghai, China). These stable NSCLC cells

expressed green fluorescent protein (GFP) and puromycin resistance gene to select stable cells for further analysis.

CCK8 and cell colony formation assays

Cells were seeded into 96-well plates at a density of 5×10^4 /mL. Then, 10 μ L of CCK8 solution (Donjindo, Japan) was added per well at the appointed time points. Absorbance at 450 nm was measured after a 2 h incubation. For cell colony formation assays, 500 cells were seeded in a 6-well plate and cultured for 2 weeks. The numbers of colonies per well were counted after staining with crystal violet. All studies were conducted with 3 replicates.

Cell cycle and apoptosis assays

For cell cycle analysis, NSCLC cells were plated into 6 well plates at 3×10^5 per well. After 24 h, cells were washed with phosphate-buffered saline (PBS) twice and trypsinized to collect cells, then cells were resuspended in cold 70% ethanol overnight. After treatment with RNase and staining with propidium iodide (PI), cell cycle position was analyzed by flow cytometry. For apoptosis assays, NSCLC cells were plated at a density of 3×10^5 per 6-well plate. After 24 h, cells were washed, collected, and stained with FITC-Annexin V, and cell apoptosis stages were analyzed by flow cytometry.

In vitro wound healing and migration assays

Cells (4×10^5) were seeded into 6-well plates. When the cells reached 95% confluence, wound healing assays were carried out with a sterile 10 μ L pipette tip to straightly scratch 3 lines through the confluent monolayer. The cells were cultured with fresh medium, and wound closure was photographed at 24, 48, and 72 h. For the migration assay, cells (5×10^4) in serum-free medium were seeded into the upper chamber of a Transwell (Merck Millipore, USA), and after 48 h, the cells in the upper chamber were removed. The number of cells that adhered to the lower membrane was imaged after staining with 0.1% crystal violet. All studies were conducted with 3 replicates.

Establishment of tumor xenografts in mice

Male 3-week-old nude mice were purchased from Guangdong Medical Laboratory Animal Center (Guangzhou, China). After acclimation for a week in individually ventilated cages (IVC), 3×10^6 cells were

subcutaneously injected into each flank (groups of LV-328-5p-m, LV-328-5p-i and LV-NC in 1 mouse). When the largest subcutaneous tumor of the mouse reached a volume of approximately 1,000 mm³, In-Vivo FX Pro (BRUKER, Germany) was applied to detect the fluorescence of subcutaneous tumors in mice. Subcutaneous tumors were resected following euthanasia, and size was calculated by tumor volume (mm³) = (L \times W²)/2. Tumor weight was recorded. This experiment was conducted in the Guangzhou Institute of Sport Science and approved by the Standards for Animal Ethics in the Guangzhou Institute of Sport Science (GZTKSGNX-2015-2) and performed in accordance with the relevant experimental animal guidelines and regulations for the care and use of animals.

MiRNA profiling and RNA deep sequencing

Candidate target genes of miR-183-5p were detected by RNA deep sequencing. Total RNA was extracted from miR-183-5p stable NSCLC cells by Trizol reagent and the RNA-seq libraries were constructed by the TruSeq RNA Library Prep Kit (Illumina). RNA-seq experiments were performed by Novel Bioinformatics Co., Ltd. (Shanghai, China, <http://www.novelbio.com/>). Data analysis was performed using NovelBio Bio-Pharm Technology for differential mRNA expression in both LV-328-5p-m and LV-328-5p-i cell lines compared with LV-NC cells.

Analysis of pathways and Gene Ontology (GO) categories

To investigate the biological roles of differentially expressed miRNA target genes, biological process GO enrichment analysis based on the GO database was performed. Kyoto Encyclopedia of Genes and Genomes (KEGG) database analysis was performed for further assessment of the signaling pathways. The interactions between miRNAs and the candidate genes were visualized by the Cytoscape open source bioinformatics software platform. Functional interactions between genes of the carcinogenesis module were annotated by the STRING database. The significant GO categories were determined by Fisher's exact test and P values were corrected by false discovery rate (FDR).

Luciferase reporter assay

For the reporter assays, miR-328-5p mimics along with pSI-check2-LOXL4-3'UTR were transfected into HEK293T cells. Lipofectamine 2000 transfection reagent (Invitrogen)

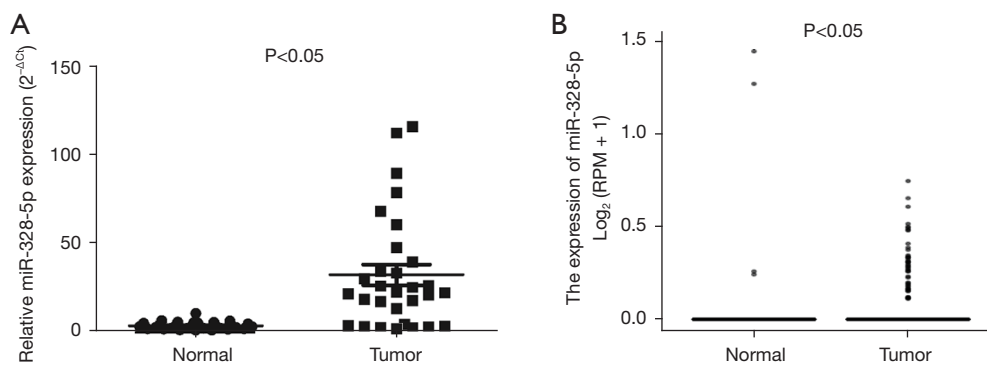


Figure 1 MiR-328-5p was upregulated in NSCLC. (A) qRT-PCR analysis of the expression of miR-328-5p in NSCLC cancer tissues and adjacent normal tissues (n=30). (B) TCGA analysis of the expression of miR-328-5p in NSCLC cancer tissues and adjacent normal tissues. NSCLC, non-small cell lung cancer; qRT-PCR, real-time quantitative polymerase chain reaction; TCGA, The Cancer Genome Atlas.

was used in this process. Luciferase activity was evaluated using a dual-luciferase reporter assay system (Promega), according to the manufacturer's instructions. Firefly luciferase activity was used for normalization.

Western blot analysis

Stably expressed NSCLC cells with or without miR-328-5p expression were collected, washed with PBS, and lysed with RIPA buffer. Equal amounts of cell lysates (20 μ g) were separated by SDS-PAGE and transferred onto PVDF (Millipore, Billerica, MA, USA) membranes. Rabbit polyclonal anti-LOXL4 (1:1,000, bs-5790R, Bioss) and mouse polyclonal anti-GAPDH (1:1,000, #5174, Cell Signaling Technology) antibodies were added to the membranes and incubated overnight at 4 $^{\circ}$ C. The anti-GAPDH antibody was used as the internal reference. The bands were exposed by ECL reagent (Thermo Fisher Scientific Inc., MA, USA) and analyzed by ImageJ software (NIH, Bethesda, MD, USA).

Statistical analysis

Statistical analysis was performed using SPSS (v. 22.0, Chicago, IL, USA). All data were presented as the mean \pm SEM. The two-tailed Student's *t*-test or analysis of variance (ANOVA) were used to compare unpaired samples. The paired Student's *t*-test was used to compare paired groups of samples. The statistical significance of all tests was defined as $P < 0.05$.

Results

Expression of miR-328-5p in lung cancer tissue and its correlation with the clinicopathological features of patients

The miR-328-5p expression level was measured by qRT-PCR in 30 NSCLC and pair-matched adjacent normal lung tissue specimens to determine whether miR-328-5p was upregulated in NSCLC. The results showed that miR-328-5p expression was significantly increased ($P < 0.05$) in NSCLC tissues relative to their matched controls (Figure 1A). Then, we used The Cancer Genome Atlas (TCGA; <https://portal.gdc.cancer.gov/>) to profile the expression of miR-328-5p in NSCLC tumor and adjacent normal tissues, which confirmed that miR-328-5p was significantly overexpressed in NSCLC samples (Figure 1B). Next, the correlation between miR-328-5p expression and clinicopathological parameters were assessed. Results showed that miR-328-5p expression levels in NSCLC were significantly associated with histological tumor type ($P < 0.05$) and differentiation ($P < 0.05$), but not with age, gender, tumor size, and TNM stage (Table 1). These results demonstrated that the over-expression of miR-328-5p might play an important role in lung cancer progression and development.

Transfection of miR-328-5p in NSCLC cell lines

In terms of the correlation between miR-328-5p expression and NSCLC progression, we further investigated the effect of miR-328-5p on the proliferation and migration abilities of NSCLC cells. NSCLC cell lines were transfected with LV-

Table 1 Correlation between the expression of miR-328-5p and the clinicopathological features of NSCLC patients (n=30)

Variable	n	MiR-328-5p expression		P value
		Low	High	
Gender				
Male	21	6	15	>0.05
Female	9	3	6	
Age, years				
≥50	17	4	13	>0.05
<50	13	3	10	
Tumor volume, mm ³				
≥5	9	2	7	>0.05
<5	21	5	16	
Pathological type				
Adenocarcinoma	18	3	15	*<0.05
Squamous cell carcinoma	12	4	8	
Differentiation degree				
High	3	2	1	*<0.05
Medium + low	27	7	20	
TNM stage				
I-II	20	5	15	>0.05
III-IV	10	3	7	

Low/high by the mean expression of miR-328-5p. Pearson χ^2 test. *, P<0.05 was considered statistically significant. NSCLC, non-small cell lung cancer.

328-5p-m, LV-328-5p-I, or LV-NC to establish the stable miR-328-5p overexpression or knockdown NSCLC cell lines. Then, the expression levels of miR-328-5p in cells were quantified *via* qRT-PCR. Compared with the expression of LV-NC cells, miR-328-5p was significantly upregulated in LV-328-5p-m transfected NSCLC cells, while LV-328-5p-i downregulated the expression of miR-328-5p (Figure 2A).

Overexpression of miR-328-5p promotes the proliferation of NSCLC cells

The role of miR-328-5p in NSCLC cell (A549 and SPC-A1) proliferation was examined by the CCK8 and colony formation assays. Results of the CCK8 assay demonstrated that overexpressed miR-328-5p significantly

promoted A549 (P<0.05) and SPC-A-1 (P<0.05) cell proliferation, while downregulation of miR-328-5p reversed the inhibitory role of miR-328-5p on A549 and SPC-A-1 cell proliferation (Figure 2B). These results were confirmed by the colony formation assay, which was used to investigate the role of miR-328-5p on NSCLC cell clonogenic survival (Figure 2C). Moreover, flow cytometry analysis revealed that overexpressing miR-328-5p could significantly promote cell cycle arrest at the G2/M phase and reduce apoptosis in NSCLC cells (Figure 2D,2E).

Overexpression of miR-328-5p promotes the migration of NSCLC cells

Considering the correlation between the expression of miR-328-5p and the progression of NSCLC, we used wound healing assays and Transwell assays in A549 and SPC-A1 cell lines transfected with either LV-328-5p-m, LV-328-5p-i, or LV-NC. As shown in Figure 3A,3B, compared with LV-NC cells, the wound healing ability and migration ability of stable miR-328-5p overexpressed cells were significantly increased. However, wound healing and migration were inhibited in NSCLC cells transfected with LV-328-5p-i compared with LV-NC cells. These results suggest that miR-183-5p can promote the migratory capacity of NSCLC cells and accelerate NSCLC progression.

MiR-328-5p promotes the tumor growth of NSCLC cells *in vivo*

To verify whether miR-328-5p could promote NSCLC tumor growth *in vivo*, nude mice received subcutaneous injections of SPC-A1 cells transfected with either LV-328-5p-m, LV-328-5p-i, or LV-NC. After 28 days, the tumor volume and weight of mice injected with LV-328-5p-m SPC-A1 cells evidently increased compared with the LV-NC group (Figure 4A,4B). Additionally, the mice injected with LV-328-5p-i SPC-A1 cells displayed significantly decreased tumor volume and weight compared with the mice injected with LV-328-5p-m SPC-A1 cells (Figure 4C). Consistent with the *in vitro* data of the present study, these data indicated that miR-328-5p promotes the tumor growth of NSCLC cells *in vivo*.

LOXLA is directly negatively regulated by miR-328-5p in NSCLC cells

To further clarify the molecular mechanisms of miR-

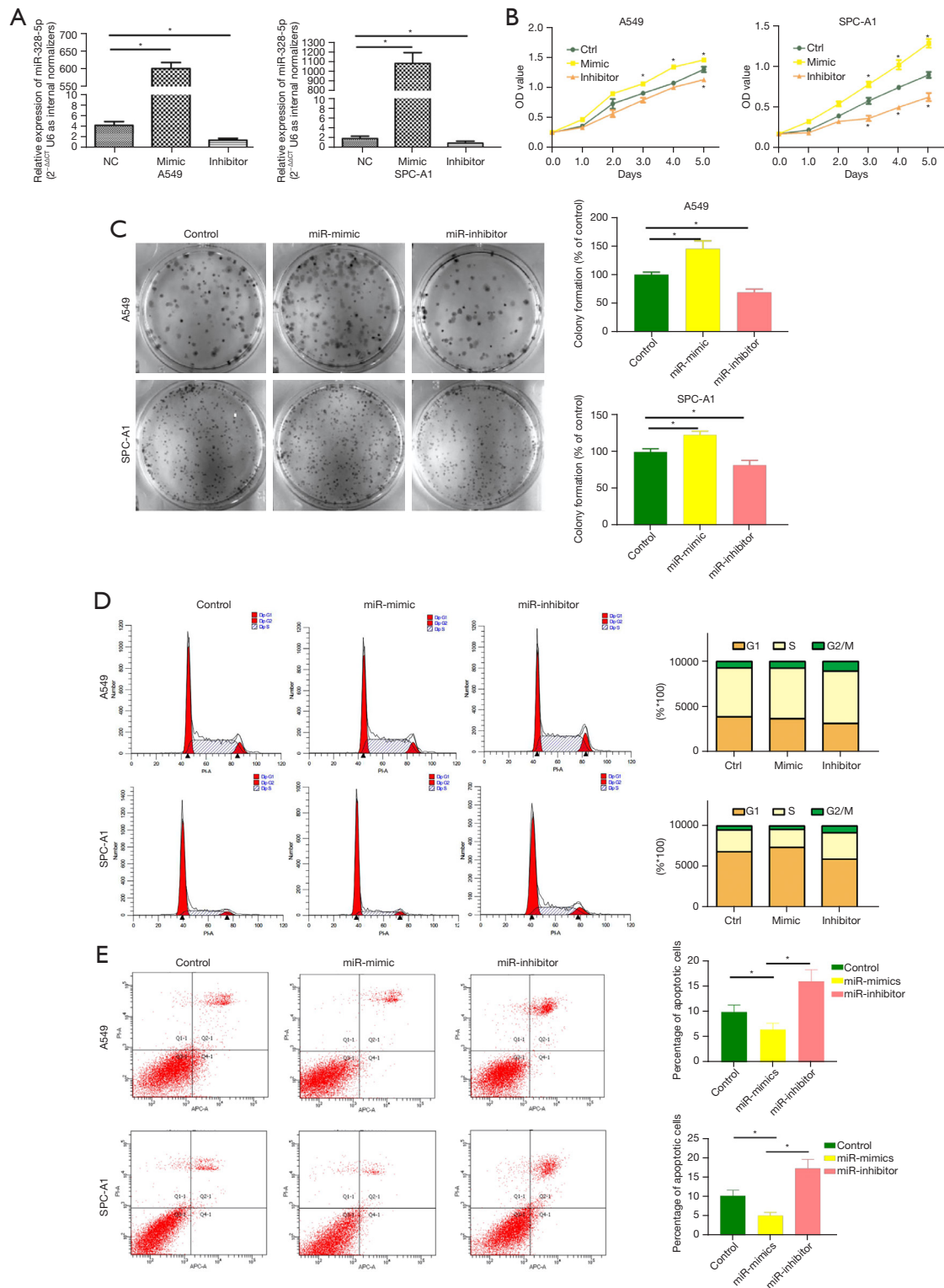


Figure 2 Overexpression of miR-328-5p promoted NSCLC cell proliferation. (A) MiR-328-5p expression in stable miR-328-5p overexpression or knockdown NSCLC cell lines. (B-E) Overexpression or knockdown of miR-328-5p in NSCLC cells affected proliferation and decreased apoptosis compared with LV-NC cells. *, P<0.05. C stained by haematoxylin. NSCLC, non-small cell lung cancer; LV-NC, lentiviral vectors negative control.

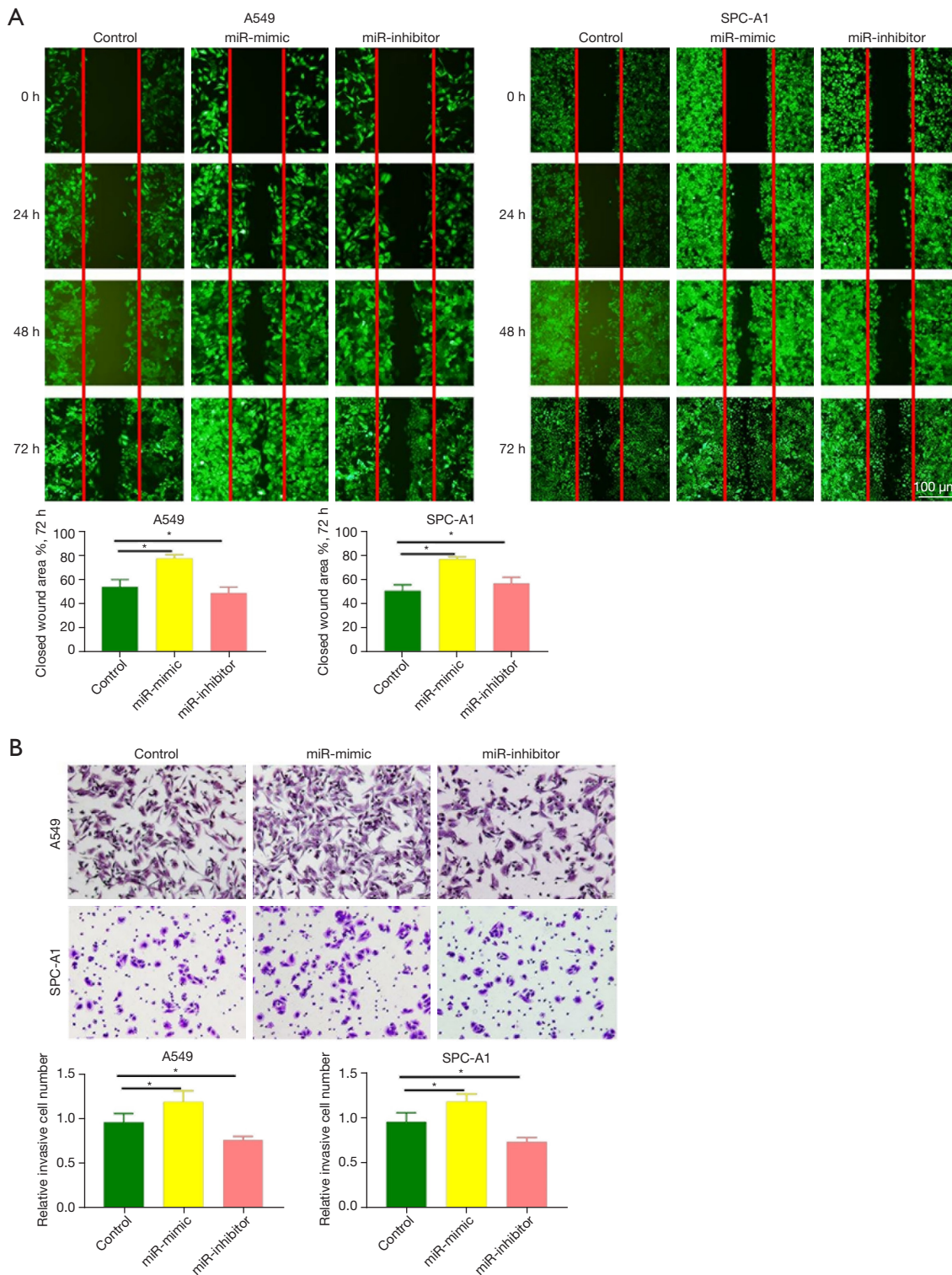


Figure 3 Overexpression of miR-328-5p promotes NSCLC cell migration. (A) the migratory ability of miR-328-5p overexpression or knockdown in NSCLC cells was measured by wound-healing assay (scale bar =500 μ m); (B) cell migration was evaluated in NSCLC cells with miR-328-5p overexpression or knockdown (dyeing with crystal violet; scale bar =100 μ m). All of the obtained cells expressed GFP. *, $P < 0.05$. NSCLC, non-small cell lung cancer; GFP, green fluorescent protein.

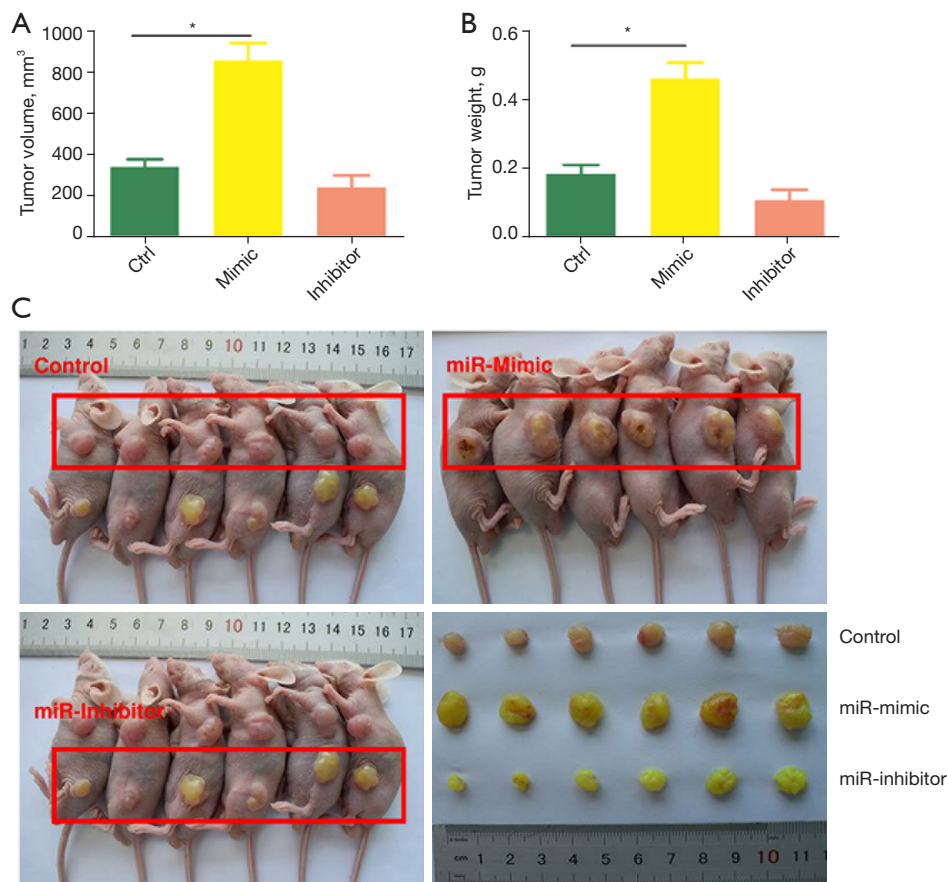


Figure 4 Overexpression of miR-328-5p promotes tumor growth in a xenograft model. (A-C) MiR-328-5p overexpression promoted tumor volume and weight in nude mice. *, $P < 0.05$.

328-5p in tumorigenesis, we overexpressed miR-328-5p and screened the downregulated differentially expressed target genes by RNA deep sequencing in NSCLC cells. A total of 14 downregulated genes were found in miR-328-5p overexpressed cells (Figure 5A). Notably, the KEGG pathways included channel activity, passive transmembrane transporter activity, ion channel complex, and copper ion binding, among others (Figure 5B-5E) (Table 2). Among the genes with several functions, we were interested in whether LOXL4, a member of the copper-dependent enzyme family, could be downregulated by miR-328-5p in NSCLC. To determine the correlation between miR-328-5p and LOXL4, luciferase reporter assays were used to determine whether miR-328-5p could recognize the 3'UTR of LOXL4 and regulate the expression of LOXL4 by their combined putative sites. Results showed that LOXL4 was able to match the intracellular miR-328-5p seed sequence at the 3'UTR region and the luciferase activity was significantly

decreased with miR-328-5p overexpression, further indicating that LOXL4 was the direct target gene of miR-328-5p (Figure 6A). A qRT-PCR assay was used to measure the expression of LOXL4 in NSCLC tissues, and the results showed that LOXL4 was obviously downregulated in both NSCLC and normal tissues (Figure 6B). Then, a western blot assay was used to evaluate the regulatory effect of miR-328-5p on LOXL4 expression in NSCLC cells. Results revealed that overexpression of miR-328-5p decreased the protein levels of LOXL4 (Figure 6C). Using UCSC XENA (<https://xenabrowser.net/datapages/>) profiling of LOXL4 expression in NSCLC tumor tissues and normal tissues, we confirmed that LOXL4 was significantly decreased in NSCLC samples. Moreover, statistical correlation analysis showed significant negative regulation between LOXL4 expression and TNM stage (TCGA, <https://portal.gdc.cancer.gov/>). Overall survival and progression-free survival were lower in NSCLC with downregulation of LOXL4,

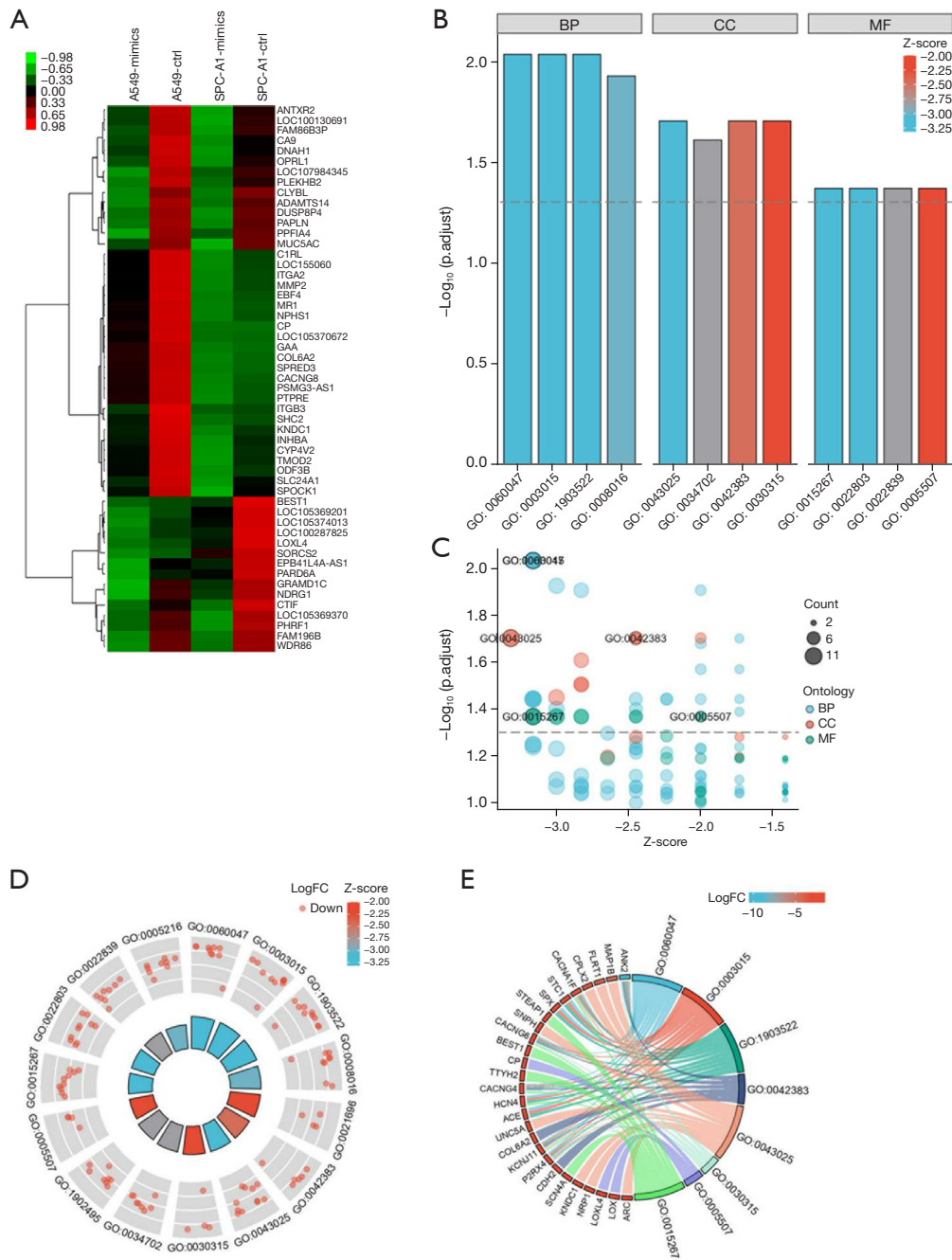


Figure 5 KEGG pathway and GO analyses of miR-328-5p overexpressing NSCLC cells. (A) Heat map of significant genes in miR-328-5p overexpressing NSCLC cells; *, $P < 0.05$ are indicated. (B-E) KEGG pathways and GO analysis of miR-328-5p overexpression. NSCLC, non-small cell lung cancer; KEGG, Kyoto Encyclopedia of Genes and Genomes; GO, Gene Ontology; BP, biological process; CC, cellular component; MF, molecular function.

Table 2 KEGG and GO analyses of miR-328-5p overexpressed NSCLC cells

Ontology	ID	Description	P _{adjust}	Gene ID
BP	GO:0060047	Heart contraction	0.0092	<i>ANK2/CACNA1F/STC1/SPX/CACNG6/CACNG4/HCN4/ACE/KCNJ11/P2RX4</i>
BP	GO:0003015	Heart process	0.0092	<i>ANK2/CACNA1F/STC1/SPX/CACNG6/CACNG4/HCN4/ACE/KCNJ11/P2RX4</i>
BP	GO:1903522	Regulation of blood circulation	0.0092	<i>ANK2/CACNA1F/STC1/SPX/CACNG6/CACNG4/HCN4/ACE/KCNJ11/P2RX4</i>
BP	GO:0008016	Regulation of heart contraction	0.0118	<i>ANK2/CACNA1F/STC1/SPX/CACNG6/CACNG4/HCN4/KCNJ11/P2RX4</i>
BP	GO:0021696	Cerebellar cortex morphogenesis	0.0124	<i>GLI1/SERPINE2/WNT7A/KNDC1</i>
BP	GO:0035637	Multicellular organismal signaling	0.0124	<i>ANK2/CACNA1F/CACNG6/CACNG4/HCN4/KCNJ11/P2RX4/SCN4A</i>
CC	GO:0042383	Sarcolemma	0.0198	<i>ANK2/CACNG6/CACNG4/COL6A2/KCNJ11/CDH2</i>
CC	GO:0043025	Neuronal cell body	0.0198	<i>MAP1B/FLRT1/CPLX2/CACNA1F/SNPH/UNC5A/KCNJ11/P2RX4/KNDC1/NRP1/ARC</i>
CC	GO:0030315	T-tubule	0.0198	<i>ANK2/CACNG6/CACNG4/KCNJ11</i>
BP	GO:0021681	Cerebellar granular layer development	0.0199	<i>SERPINE2/WNT7A/KNDC1</i>
BP	GO:0021587	Cerebellum morphogenesis	0.0209	<i>GLI1/SERPINE2/WNT7A/KNDC1</i>
CC	GO:0034702	Ion channel complex	0.0246	<i>CACNA1F/CACNG6/BEST1/TTYH2/CACNG4/HCN4/KCNJ11/SCN4A</i>
BP	GO:0021575	Hindbrain morphogenesis	0.0269	<i>GLI1/SERPINE2/WNT7A/KNDC1</i>
BP	GO:1900451	Positive regulation of glutamate receptor signaling pathway	0.0269	<i>NECAB2/CACNG4/ARC</i>
CC	GO:1902495	Transmembrane transporter complex	0.0312	<i>CACNA1F/CACNG6/BEST1/TTYH2/CACNG4/HCN4/KCNJ11/SCN4A</i>
CC	GO:1990351	Transporter complex	0.0312	<i>CACNA1F/CACNG6/BEST1/TTYH2/CACNG4/HCN4/KCNJ11/SCN4A</i>
CC	GO:0097060	Synaptic membrane	0.0354	<i>ANK2/SNPH/CACNG4/DLG5/CDH2/DNAJA3/GRM4/NRP1/ARC</i>
BP	GO:0021695	Cerebellar cortex development	0.0361	<i>GLI1/SERPINE2/WNT7A/KNDC1</i>
BP	GO:0051899	Membrane depolarization	0.0361	<i>ANK2/CACNG4/HCN4/P2RX4/SCN4A</i>
BP	GO:0043062	Extracellular structure organization	0.0361	<i>RAMP2/ITGAM/LPL/ADAMTS14/NPHS1/ECM2/COL6A2/THSD4/LOXL4/LOX</i>
BP	GO:0051047	Positive regulation of secretion	0.0361	<i>CD33/ITGAM/LPL/TNFRSF14/OPRL1/INHBA/CD177/EXPH5/TWIST1/P2RX4</i>
BP	GO:0061337	Cardiac conduction	0.0361	<i>ANK2/CACNA1F/CACNG6/CACNG4/HCN4/KCNJ11</i>
BP	GO:0006816	Calcium ion transport	0.0361	<i>CD33/ANK2/RAMP2/CACNA1F/STC1/OPRL1/CACNG6/BEST1/CACNG4/P2RX4</i>
BP	GO:0050804	Modulation of chemical synaptic transmission	0.0361	<i>MAP1B/CPLX2/CACNG4/SERPINE2/CDH2/WNT7A/GRM4/EGR2/MCTP1/ARC</i>
BP	GO:0099177	Regulation of trans-synaptic signaling	0.0361	<i>MAP1B/CPLX2/CACNG4/SERPINE2/CDH2/WNT7A/GRM4/EGR2/MCTP1/ARC</i>
BP	GO:0006942	Regulation of striated muscle contraction	0.0361	<i>ANK2/STC1/HCN4/P2RX4/SCN4A</i>
BP	GO:0044342	Type B pancreatic cell proliferation	0.0361	<i>NUPR1/IGFBP3/SGPP2</i>
BP	GO:0045216	Cell-cell junction organization	0.0397	<i>ANK2/RAMP2/CD177/ACE/DLG5/CDH2</i>

Table 2 (continued)

Table 2 (continued)

Ontology	ID	Description	P _{adjust}	Gene ID
BP	GO:0030198	Extracellular matrix organization	0.0397	RAMP2/ITGAM/ADAMTS14/NPHS1/ECM2/COL6A2/THSD4/LOXL4/LOX
BP	GO:0044062	Regulation of excretion	0.0409	STC1/SPX/NPHS1
MF	GO:0005507	Copper ion binding	0.0428	CP/P2RX4/LOXL4/LOX
MF	GO:0015267	Channel activity	0.0428	CACNA1F/STEAP1/CACNG6/BEST1/TTYH2/CACNG4/HCN4/KCNJ11/P2RX4/SCN4A
MF	GO:0022803	Passive transmembrane transporter activity	0.0428	CACNA1F/STEAP1/CACNG6/BEST1/TTYH2/CACNG4/HCN4/KCNJ11/P2RX4/SCN4A
MF	GO:0022839	Ion gated channel activity	0.0428	CACNA1F/CACNG6/TTYH2/CACNG4/HCN4/KCNJ11/P2RX4/SCN4A
MF	GO:0005216	Ion channel activity	0.0428	CACNA1F/CACNG6/BEST1/TTYH2/CACNG4/HCN4/KCNJ11/P2RX4/SCN4A
MF	GO:0022836	Gated channel activity	0.0428	CACNA1F/CACNG6/TTYH2/CACNG4/HCN4/KCNJ11/P2RX4/SCN4A
MF	GO:0022838	Substrate-specific channel activity	0.0428	CACNA1F/CACNG6/BEST1/TTYH2/CACNG4/HCN4/KCNJ11/P2RX4/SCN4A
MF	GO:0005244	Voltage-gated ion channel activity	0.0428	CACNA1F/CACNG6/CACNG4/HCN4/KCNJ11/SCN4A
MF	GO:0022832	Voltage-gated channel activity	0.0428	CACNA1F/CACNG6/CACNG4/HCN4/KCNJ11/SCN4A
BP	GO:0016358	Dendrite development	0.0505	MAP1B/FLRT1/DLG5/WNT7A/KNDC1/NRP1/ARC
MF	GO:0022843	Voltage-gated cation channel activity	0.0518	CACNA1F/CACNG6/CACNG4/HCN4/KCNJ11
CC	GO:0034703	Cation channel complex	0.0523	CACNA1F/CACNG6/CACNG4/HCN4/KCNJ11/SCN4A
CC	GO:0005891	Voltage-gated calcium channel complex	0.0523	CACNA1F/CACNG6/CACNG4
CC	GO:1990454	L-type voltage-gated calcium channel complex	0.0523	CACNG6/CACNG4
BP	GO:0006937	Regulation of muscle contraction	0.0551	ANK2/STC1/SPX/HCN4/P2RX4/SCN4A
BP	GO:0034765	Regulation of ion transmembrane transport	0.0564	ANK2/CACNA1F/OPRL1/CACNG6/CACNG4/HCN4/KCNJ11/TWIST1/SCN4A/ARC
BP	GO:0070838	Divalent metal ion transport	0.0564	CD33/ANK2/RAMP2/CACNA1F/STC1/OPRL1/CACNG6/BEST1/CACNG4/P2RX4
BP	GO:0021602	Cranial nerve morphogenesis	0.0577	GLI3/NRP1/EGR2
BP	GO:0072511	Divalent inorganic cation transport	0.0577	CD33/ANK2/RAMP2/CACNA1F/STC1/OPRL1/CACNG6/BEST1/CACNG4/P2RX4
BP	GO:0050808	Synapse organization	0.0587	ITGAM/MAP1B/FLRT1/DLG5/CDH2/DNAJA3/WNT7A/NRP1/ARC
BP	GO:0008217	Regulation of blood pressure	0.0587	RAMP2/SPX/OPRL1/ACE/P2RX4/NPR3
BP	GO:0021953	Central nervous system neuron differentiation	0.0587	INHBA/GLI3/CHD5/WNT7A/KNDC1/NRP1
BP	GO:0051966	Regulation of synaptic transmission, glutamatergic	0.0587	CACNG4/SERPINE2/CDH2/GRM4
BP	GO:2001259	Positive regulation of cation channel activity	0.0587	ANK2/CACNG4/KCNJ11/ARC
BP	GO:0007043	Cell-cell junction assembly	0.0610	ANK2/RAMP2/ACE/DLG5/CDH2
BP	GO:0048167	Regulation of synaptic plasticity	0.0610	MAP1B/CPLX2/SERPINE2/EGR2/MCTP1/ARC
CC	GO:0045211	Postsynaptic membrane	0.0636	ANK2/CACNG4/DLG5/CDH2/DNAJA3/NRP1/ARC

Table 2 (continued)

Table 2 (continued)

Ontology	ID	Description	P _{adjust}	Gene ID
CC	GO:0014704	Intercalated disc	0.0636	ANK2/KCNJ11/CDH2
MF	GO:0031404	Chloride ion binding	0.0646	ACE/NPR3
MF	GO:0005245	Voltage-gated calcium channel activity	0.0646	CACNA1F/CACNG6/CACNG4
MF	GO:0017046	Peptide hormone binding	0.0646	RAMP2/INHBA/NPR3
MF	GO:0005261	Cation channel activity	0.0646	CACNA1F/CACNG6/CACNG4/HCN4/KCNJ11/P2RX4/SCN4A
MF	GO:0042562	Hormone binding	0.0646	RAMP2/INHBA/ALDH1A1/NPR3
MF	GO:0004029	Aldehyde dehydrogenase (NAD) activity	0.0646	ALDH1L2/ALDH1A1
MF	GO:0008201	Heparin binding	0.0646	LPL/LTBP2/ECM2/SERPINE2/NRP1
MF	GO:0016641	Oxidoreductase activity, acting on the CH-NH2 group of donors, oxygen as acceptor	0.0661	LOXL4/LOX
BP	GO:0003002	Regionalization	0.0765	ITGAM/NBL1/GLI1/GLI3/WNT7A/NRP1/EGR2/ARC
BP	GO:0008589	Regulation of smoothed signaling pathway	0.0765	GLI1/SERPINE2/GLI3/DLG5
BP	GO:0050866	Negative regulation of cell activation	0.0765	IL13RA2/TNFRSF14/INHBA/SERPINE2/GLI3/DLG5
BP	GO:0032355	Response to estradiol	0.0765	RAMP2/MAP1B/OPRL1/KCNJ11/WNT7A
BP	GO:0021675	Nerve development	0.0765	SERPINE2/GLI3/NRP1/EGR2
BP	GO:0086010	Membrane depolarization during action potential	0.0796	ANK2/HCN4/SCN4A
BP	GO:0007389	Pattern specification process	0.0796	ITGAM/NBL1/STC1/GLI1/GLI3/WNT7A/NRP1/EGR2/ARC
BP	GO:0055117	Regulation of cardiac muscle contraction	0.0819	ANK2/STC1/HCN4/P2RX4
BP	GO:0086070	SA node cell to atrial cardiac muscle cell communication	0.0835	ANK2/HCN4
BP	GO:0150063	Visual system development	0.0835	ITGAM/INHBA/GLI3/TWIST1/CRYGN/WNT7A/CRYBA2/NRP1
BP	GO:0048880	Sensory system development	0.0852	ITGAM/INHBA/GLI3/TWIST1/CRYGN/WNT7A/CRYBA2/NRP1
BP	GO:0034330	Cell junction organization	0.0852	ANK2/RAMP2/CD177/ACE/DLG5/CDH2/NRP1
BP	GO:0021561	Facial nerve development	0.0852	NRP1/EGR2
BP	GO:0021604	Cranial nerve structural organization	0.0852	NRP1/EGR2
BP	GO:0021610	Facial nerve morphogenesis	0.0852	NRP1/EGR2
BP	GO:0031915	Positive regulation of synaptic plasticity	0.0852	MAP1B/CPLX2
BP	GO:1902563	Regulation of neutrophil activation	0.0852	ITGAM/CD177
BP	GO:0017157	Regulation of exocytosis	0.0852	IL13RA2/ITGAM/CPLX2/CD177/EXPH5/WNT7A
BP	GO:0007409	Axonogenesis	0.0852	MAP1B/GLI3/CRMP1/UNC5A/EPHA10/CDH2/WNT7A/NRP1/EGR2
BP	GO:0060021	Roof of mouth development	0.0852	INHBA/GLI3/TWIST1/WNT7A
BP	GO:0007584	Response to nutrient	0.0852	MAP1B/LPL/STC1/CYP24A1/KCNJ11/P2RX4

Table 2 (continued)

Table 2 (continued)

Ontology	ID	Description	P _{adjust}	Gene ID
BP	GO:0030900	Forebrain development	0.0852	<i>ITGAM/GLI1/INHBA/GLI3/CHD5/CDH2/WNT7A/NRP1</i>
BP	GO:0009953	Dorsal/ventral pattern formation	0.0860	<i>NBL1/GLI1/GLI3/WNT7A</i>
BP	GO:0086004	Regulation of cardiac muscle cell contraction	0.0875	<i>ANK2/STC1/HCN4</i>
BP	GO:0030902	Hindbrain development	0.0875	<i>GLI1/SERPINE2/WNT7A/KNDC1/EGR2</i>
BP	GO:0060019	Radial glial cell differentiation	0.0892	<i>GLI3/CDH2</i>
BP	GO:0001649	Osteoblast differentiation	0.0894	<i>GLI1/GLI3/CYP24A1/TWIST1/IGFBP3/LOX</i>
BP	GO:0035249	Synaptic transmission, glutamatergic	0.0894	<i>CACNG4/SERPINE2/CDH2/GRM4</i>
MF	GO:0005248	Voltage-gated sodium channel activity	0.0895	<i>HCN4/SCN4A</i>
MF	GO:0016638	Oxidoreductase activity, acting on the CH-NH2 group of donors	0.0895	<i>LOXL4/LOX</i>
MF	GO:0005179	Hormone activity	0.0895	<i>STC1/SPX/INHBA/INHBE</i>
MF	GO:0005262	Calcium channel activity	0.0895	<i>CACNA1F/CACNG6/CACNG4/P2RX4</i>
BP	GO:0043271	Negative regulation of ion transport	0.0909	<i>CD33/STC1/OPRL1/SERPINE2/TWIST1</i>
BP	GO:0043300	Regulation of leukocyte degranulation	0.0909	<i>IL13RA2/ITGAM/CD177</i>
BP	GO:0001503	Ossification	0.0909	<i>STC1/GLI1/GLI3/CYP24A1/TWIST1/IGFBP3/EGR2/LOX</i>
BP	GO:0003084	Positive regulation of systemic arterial blood pressure	0.0909	<i>SPX/ACE</i>
BP	GO:0043116	Negative regulation of vascular permeability	0.0909	<i>RAMP2/MIR23A</i>
BP	GO:0061029	Eyelid development in camera-type eye	0.0909	<i>INHBA/TWIST1</i>
BP	GO:0061469	Regulation of type B pancreatic cell proliferation	0.0909	<i>NUPR1/SGPP2</i>
BP	GO:1903532	Positive regulation of secretion by cell	0.0909	<i>CD33/ITGAM/LPL/TNFRSF14/INHBA/CD177/EXPH5/TWIST1</i>
BP	GO:1903305	Regulation of regulated secretory pathway	0.0909	<i>IL13RA2/ITGAM/CPLX2/CD177/WNT7A</i>
BP	GO:0043010	Camera-type eye development	0.0909	<i>INHBA/GLI3/TWIST1/CRYGN/WNT7A/CRYBA2/NRP1</i>
BP	GO:1903115	Regulation of actin filament-based movement	0.0909	<i>ANK2/STC1/HCN4</i>
BP	GO:0099173	Postsynapse organization	0.0951	<i>CDH2/DNAJA3/WNT7A/NRP1/ARC</i>
BP	GO:0007215	Glutamate receptor signaling pathway	0.0967	<i>NECAB2/CACNG4/GRM4/ARC</i>
BP	GO:0035810	Positive regulation of urine volume	0.0970	<i>OPRL1/NPR3</i>
MF	GO:0019955	Cytokine binding	0.0982	<i>IL13RA2/NBL1/TNFRSF14/NRP1</i>
BP	GO:0034329	Cell junction assembly	0.0999	<i>ANK2/RAMP2/ACE/DLG5/CDH2/NRP1</i>
BP	GO:0021549	Cerebellum development	0.0999	<i>GLI1/SERPINE2/WNT7A/KNDC1</i>

KEGG, Kyoto Encyclopedia of Genes and Genomes; GO, Gene Ontology; NSCLC, non-small cell lung cancer; BP, biological process; MF, molecular function; CC, cellular component.

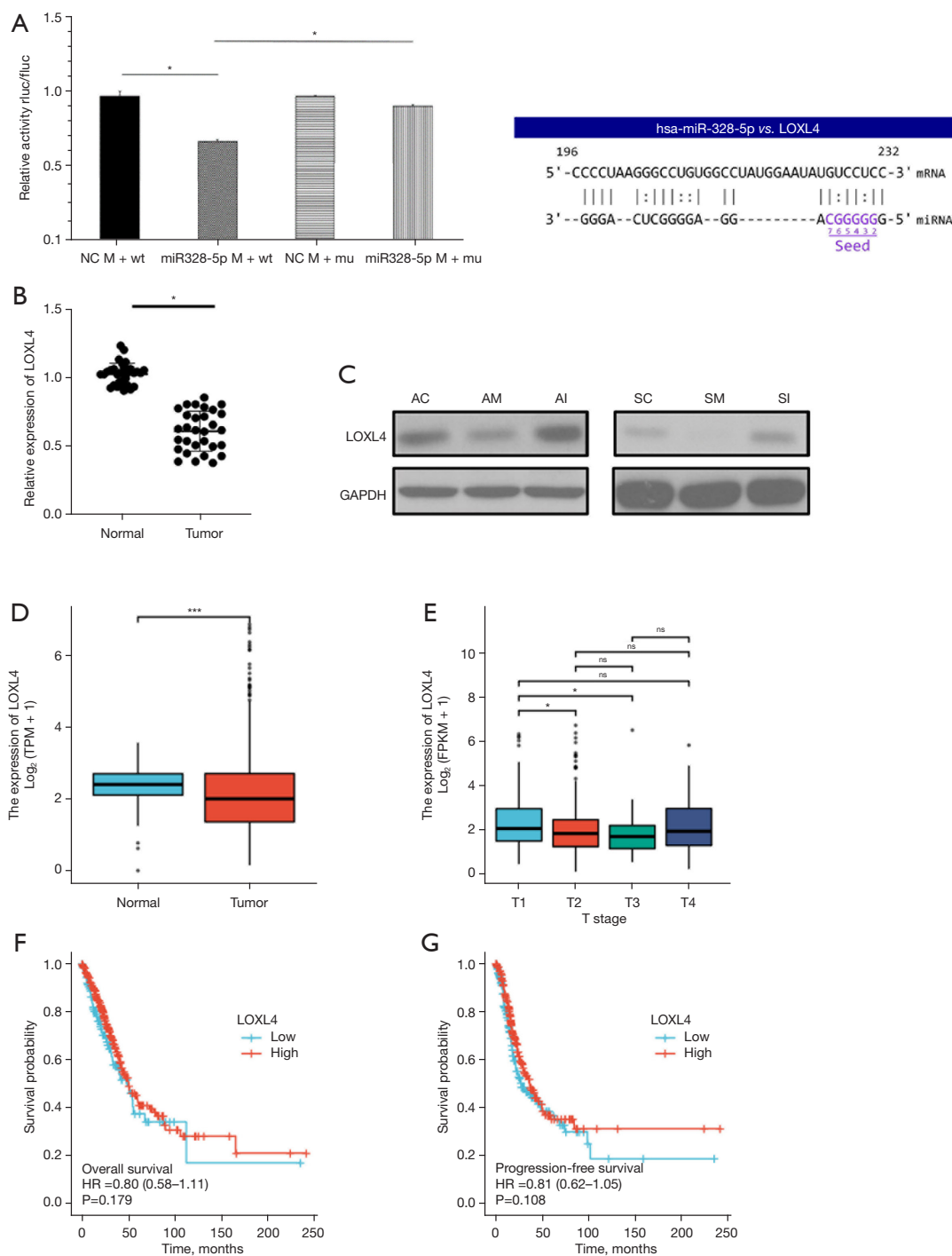


Figure 6 LOXL4 is a direct target of miR-328-5p. (A) The luciferase reporter assay showed the interaction of miR-328-5p and LOXL4 3'UTR. *, $P < 0.05$. The binding site between miR-328-5p and LOXL4 was exhibited. (B) The gene expression of LOXL4 in NSCLC tumor tissues and adjacent normal tissues was measured by qRT-PCR. *, $P < 0.05$. (C) The protein expression of LOXL4 in NSCLC cells was measured by western blot. (D) TCGA analysis of the expression of LOXL4 in NSCLC cancer tissues and adjacent normal tissues. ***, $P < 0.001$. (E-G) Log-rank test and Kaplan-Meier survival curve were used to evaluate the T stage, overall survival, and progression-free survival. *, $P < 0.05$; ns, $P > 0.05$. LOXL4, lysyl oxidase like 4; NSCLC, non-small cell lung cancer; TCGA, The Cancer Genome Atlas; qRT-PCR, real-time quantitative polymerase chain reaction.

but showed no significant difference (Figure 6D-6G). These data indicate that overexpressed miR-328-5p in NSCLC interacted with LOXL4.

Discussion

In this experimental and clinical study, we found that the progression of NSCLC is closely related to the expression of miR-328-5p. Overexpressed miR-328-5p could promote the proliferation and migration of NSCLC cells and promote tumor growth in nude mice. This indicated that high expression of miR-328-5p is a high-risk factor in NSCLC. Furthermore, according to miRNA deep sequencing and KEGG pathway/GO analysis categories, we found that overexpression of miR-328-5p inhibited LOXL4 expression and was significantly correlated with the proliferation and migration of NSCLC cells. These results showed that, in NSCLC, miR-328-5p is a novel tumor suppressor by targeting LOXL4.

With a high incidence and poor survival rates, NSCLC has been the leading cause of cancer-associated mortality worldwide (1,2,17). NSCLC can be divided into 2 major categories, namely squamous cell carcinoma and adenocarcinoma. Although chemotherapy, molecular targeted therapy, and immunotherapy have made promising advances in NSCLC treatment, the overall clinical outcomes are poor, with poor prognosis and increased risk of treatment-related complications (4,18,19). Thus, there is an urgent need to find novel diagnostic and prognostic biomarkers for NSCLC.

Serving as essential regulators in tumorigenesis and tumor development, miRNAs can regulate different tumor processes, including initiation, promotion, malignant conversion, progression, and metastasis (20,21). Aberrant miRNA expression levels are promising and novel makers for tumor diagnosis (22), prognosis (23), and treatment (24,25). Emerging evidence demonstrates that miRNAs play important roles in the pathogenesis of lung cancer (26-28). MiR-151a could promote cell proliferation and migration by regulating E-cadherin in lung cancer (29). Overexpression of miR-1275 could target HIF-1 α and resulted in shorter overall survival and recurrence-free survival in NSCLC (27). In this study, we found that miR-328-5p was overexpressed in NSCLC, and was significantly associated with histological tumor type and differentiation. Additionally, overexpression of miR-328-5p significantly promoted cell proliferation and migration. These results suggest that miR-328-5p acts as a crucial tumor promoter

in NSCLC carcinogenesis.

MiRNAs exert their numerous functional roles by their specific interactions with upregulated or downregulated mRNAs of target genes (30). In order to investigate the target gene regulated by miR-328-5p, we used high throughput sequencing to screen out the differentially expressed genes. Based on sequencing data for target genes in miR-328-5p overexpressed cells, we found that 11 genes were significantly downregulated. These potential target genes and the analysis of several key pathways showed that miR-328-5p may be involved in pathways such as channel activity, passive transmembrane transporter activity, ion channel complex, and copper ion binding, among others. Lysyl oxidases (LOX) are a family of copper-dependent enzymes comprised of 5 paralogues: the prototypical LOX and 4 LOX-like (LOXL) enzymes labeled 1 through 4 (31). The main function of the LOX family (LOX, LOXL1, LOXL2, LOXL3, and LOXL4) is to cross-link collagen and elastin, shaping the structure and strength of the extracellular matrix (ECM) (32). LOXL4 is widely expressed *in vivo*. So far, the role of LOXL4 in human malignancies is scarcely understood. Recent studies showed that LOXL4 has both tumor oncogenic and tumor suppressor roles (33,34). Researchers found that LOXL4 was significantly correlated with breast cancer (24), gastric cancer (35), and hepatocellular carcinoma (33), whereas it acts as a tumor suppressor in lung cancer (34) and bladder cancer (36). However, the roles and mechanisms of LOXL4 in NSCLC remain unclear. In the present study, we assessed the correlation between LOXL4 expression and the clinicopathological characteristics of NSCLC patients. We found significantly lower expression of LOXL4 in NSCLC tumor tissues than in normal tissues. Moreover, we found that LOXL4 expression was correlated with the TNM stage, but had a low correlation with overall survival and progression-free survival in NSCLC patients.

In summary, we found that miR-328-5p overexpression promoted cell proliferation and migration, and can be defined as a crucial tumor promoter by downregulating LOXL4 expression in NSCLC. These results suggest that miR-328-5p may serve as a predictive marker for prognosis, as well as a therapeutic target for NSCLC patients.

Acknowledgments

Funding: This work was supported by the National Science Foundation of China (Nos. 81673840, 81803877,

81873205); the Natural Science Foundation of Guangdong Province, China (No. 2020B1515120063); the Guangdong Basic and Applied Basic Research Foundation, China (No. 2020A1515110651); Social science and Technology Development Foundation of Dongguan (No. 202050715001207); Medical Scientific Research Foundation of Guangdong Province, China (No. 20201151015201); and the Innovation Team and Talents Cultivation Program of National Administration of Traditional Chinese Medicine (No. ZYYCXTD-C-202001).

Footnote

Reporting Checklist: The authors have completed the ARRIVE reporting checklist. Available at <https://atm.amegroups.com/article/view/10.21037/atm-22-345/rc>

Data Sharing Statement: Available at <https://atm.amegroups.com/article/view/10.21037/atm-22-345/dss>

Conflicts of Interest: All authors have completed the ICMJE uniform disclosure form (available at <https://atm.amegroups.com/article/view/10.21037/atm-22-345/coif>). The authors have no conflicts of interest to declare.

Ethical Statement: The authors are accountable for all aspects of the work in ensuring that questions related to the accuracy or integrity of any part of the work are appropriately investigated and resolved. The study was conducted in accordance with the Declaration of Helsinki (as revised in 2013). The study was approved by the Ethics Committee of Nanfang Hospital and informed consent was taken from all the patients. Animal experiment was approved by the Standards for Animal Ethics in the Guangzhou Institute of Sport Science (No. GZTKSGNX-2015-2) and performed in accordance with the relevant experimental animal guidelines and regulations for the care and use of animals.

Open Access Statement: This is an Open Access article distributed in accordance with the Creative Commons Attribution-NonCommercial-NoDerivs 4.0 International License (CC BY-NC-ND 4.0), which permits the non-commercial replication and distribution of the article with the strict proviso that no changes or edits are made and the original work is properly cited (including links to both the formal publication through the relevant DOI and the license). See: <https://creativecommons.org/licenses/by-nc-nd/4.0/>.

References

- Liu Y, Fan J, Xu T, et al. Extracellular vesicle tetraspanin-8 level predicts distant metastasis in non-small cell lung cancer after concurrent chemoradiation. *Sci Adv* 2020;6:eaz6162.
- Siegel RL, Miller KD, Jemal A. Cancer statistics, 2018. *CA Cancer J Clin* 2018;68:7-30.
- Okuyama A. Lung cancer incidence rates in the world from the Cancer Incidence in Five Continents XI. *Jpn J Clin Oncol* 2018;48:300-1.
- Sullivan DR, Forsberg CW, Ganzini L, et al. Longitudinal Changes in Depression Symptoms and Survival Among Patients With Lung Cancer: A National Cohort Assessment. *J Clin Oncol* 2016;34:3984-91.
- Cao M, Chen W. Epidemiology of lung cancer in China. *Thorac Cancer* 2019;10:3-7.
- Feng RM, Zong YN, Cao SM, et al. Current cancer situation in China: good or bad news from the 2018 Global Cancer Statistics? *Cancer Commun (Lond)* 2019;39:22.
- Martín-Sánchez JC, Lunet N, González-Marrón A, et al. Projections in Breast and Lung Cancer Mortality among Women: A Bayesian Analysis of 52 Countries Worldwide. *Cancer Res* 2018;78:4436-42.
- Zeng F, Wang Q, Wang S, et al. Linc00173 promotes chemoresistance and progression of small cell lung cancer by sponging miR-218 to regulate Etk expression. *Oncogene* 2020;39:293-307.
- Pan J, Fang S, Tian H, et al. lncRNA JPX/miR-33a-5p/Twist1 axis regulates tumorigenesis and metastasis of lung cancer by activating Wnt/ β -catenin signaling. *Mol Cancer* 2020;19:9.
- Xu Y, Lin J, Jin Y, et al. The miRNA hsa-miR-6515-3p potentially contributes to lncRNA H19-mediated-lung cancer metastasis. *J Cell Biochem* 2019;120:17413-21.
- Zhang L, Lin J, Ye Y, et al. Serum MicroRNA-150 Predicts Prognosis for Early-Stage Non-Small Cell Lung Cancer and Promotes Tumor Cell Proliferation by Targeting Tumor Suppressor Gene SRCIN1. *Clin Pharmacol Ther* 2018;103:1061-73.
- Gallach S, Jantus-Lewintre E, Calabuig-Fariñas S, et al. MicroRNA profiling associated with non-small cell lung cancer: next generation sequencing detection, experimental validation, and prognostic value. *Oncotarget* 2017;8:56143-57.
- Saul MJ, Hegewald AB, Emmerich AC, et al. Mass Spectrometry-Based Proteomics Approach Characterizes the Dual Functionality of miR-328 in Monocytes. *Front*

- Pharmacol 2019;10:640.
14. Delic S, Lottmann N, Stelzl A, et al. MiR-328 promotes glioma cell invasion via SFRP1-dependent Wnt-signaling activation. *Neuro Oncol* 2014;16:179-90.
 15. Yin Y, Castro AM, Hoekstra M, et al. Fibroblast Growth Factor 9 Regulation by MicroRNAs Controls Lung Development and Links DICER1 Loss to the Pathogenesis of Pleuropulmonary Blastoma. *PLoS Genet* 2015;11:e1005242.
 16. Arora S, Ranade AR, Tran NL, et al. MicroRNA-328 is associated with (non-small) cell lung cancer (NSCLC) brain metastasis and mediates NSCLC migration. *Int J Cancer* 2011;129:2621-31.
 17. Smeltzer MP, Lee YS, Faris M Div NR, et al. Trends in Accuracy and Comprehensiveness of Pathology Reports for Resected NSCLC in a High Mortality Area of the United States. *J Thorac Oncol* 2021;16:1663-71.
 18. Borzi C, Ganzinelli M, Caiola E, et al. LKB1 Down-Modulation by miR-17 Identifies Patients With NSCLC Having Worse Prognosis Eligible for Energy-Stress-Based Treatments. *J Thorac Oncol* 2021;16:1298-311.
 19. Nishio M, Barlesi F, West H, et al. Atezolizumab Plus Chemotherapy for First-Line Treatment of Nonsquamous NSCLC: Results From the Randomized Phase 3 IMpower132 Trial. *J Thorac Oncol* 2021;16:653-64.
 20. Zhang B, Pan X, Cobb GP, et al. microRNAs as oncogenes and tumor suppressors. *Dev Biol* 2007;302:1-12.
 21. Yu L, Sui B, Fan W, et al. Exosomes derived from osteogenic tumor activate osteoclast differentiation and concurrently inhibit osteogenesis by transferring COL1A1-targeting miRNA-92a-1-5p. *J Extracell Vesicles* 2021;10:e12056.
 22. Zhang YH, Jin M, Li J, et al. Identifying circulating miRNA biomarkers for early diagnosis and monitoring of lung cancer. *Biochim Biophys Acta Mol Basis Dis* 2020;1866:165847.
 23. Zhang J, Lou W. A Key mRNA-miRNA-lncRNA Competing Endogenous RNA Triple Sub-network Linked to Diagnosis and Prognosis of Hepatocellular Carcinoma. *Front Oncol* 2020;10:340.
 24. Yin H, Wang Y, Wu Y, et al. EZH2-mediated Epigenetic Silencing of miR-29/miR-30 targets LOXL4 and contributes to Tumorigenesis, Metastasis, and Immune Microenvironment Remodeling in Breast Cancer. *Theranostics* 2020;10:8494-512.
 25. Sharma P, Dando I, Strippoli R, et al. Nanomaterials for Autophagy-Related miRNA-34a Delivery in Cancer Treatment. *Front Pharmacol* 2020;11:1141.
 26. Fehlmann T, Kahraman M, Ludwig N, et al. Evaluating the Use of Circulating MicroRNA Profiles for Lung Cancer Detection in Symptomatic Patients. *JAMA Oncol* 2020;6:714-23.
 27. Jiang N, Zou C, Zhu Y, et al. HIF-1 α -regulated miR-1275 maintains stem cell-like phenotypes and promotes the progression of LUAD by simultaneously activating Wnt/ β -catenin and Notch signaling. *Theranostics* 2020;10:2553-70.
 28. Zhong S, Golpon H, Zardo P, et al. miRNAs in lung cancer. A systematic review identifies predictive and prognostic miRNA candidates for precision medicine in lung cancer. *Transl Res* 2021;230:164-96.
 29. Daugaard I, Sanders KJ, Idica A, et al. miR-151a induces partial EMT by regulating E-cadherin in NSCLC cells. *Oncogenesis* 2017;6:e366.
 30. Nikolic I, Elsworth B, Dodson E, et al. Discovering cancer vulnerabilities using high-throughput microRNA screening. *Nucleic Acids Res* 2017;45:12657-70.
 31. Rodriguez-Pascual F, Rosell-Garcia T. Lysyl Oxidases: Functions and Disorders. *J Glaucoma* 2018;27 Suppl 1:S15-9.
 32. Lucero HA, Kagan HM. Lysyl oxidase: an oxidative enzyme and effector of cell function. *Cell Mol Life Sci* 2006;63:2304-16.
 33. Li R, Wang Y, Zhang X, et al. Exosome-mediated secretion of LOXL4 promotes hepatocellular carcinoma cell invasion and metastasis. *Mol Cancer* 2019;18:18.
 34. Zhang Y, Jiang WL, Yang JY, et al. Downregulation of lysyl oxidase-like 4 LOXL4 by miR-135a-5p promotes lung cancer progression in vitro and in vivo. *J Cell Physiol* 2019;234:18679-87.
 35. Li RK, Zhao WY, Fang F, et al. Lysyl oxidase-like 4 (LOXL4) promotes proliferation and metastasis of gastric cancer via FAK/Src pathway. *J Cancer Res Clin Oncol* 2015;141:269-81.
 36. Wu G, Guo Z, Chang X, et al. LOXL1 and LOXL4 are epigenetically silenced and can inhibit ras/extracellular signal-regulated kinase signaling pathway in human bladder cancer. *Cancer Res* 2007;67:4123-9.

Cite this article as: Ji Y, You Y, Wu Y, Wang M, He Q, Zhou X, Chen L, Sun X, Liu Y, Fu X, Kwan HY, Zuo Q, Luo R, Zhao X. Overexpression of miR-328-5p influences cell growth and migration to promote NSCLC progression by targeting LOXL4. *Ann Transl Med* 2022;10(6):301. doi: 10.21037/atm-22-345